Earth, Planets and Space
a SpringerOpen Journal

FRONTIER LETTER Open Access

# Frictional properties of sediments entering the Costa Rica subduction zone offshore the Osa Peninsula: implications for fault slip in shallow subduction zones

Yuka Namiki[1], Akito Tsutsumi[1*], Kohtaro Ujiie[2,3] and Jun Kameda[4]

## Abstract

We examined the frictional properties of sediments on the Cocos plate offshore the Osa Peninsula, Costa Rica, and explored variations in the intrinsic frictional properties of the sediment inputs to the Costa Rica subduction zone. Sediment samples were collected at Site U1381A during the Integrated Ocean Drilling Program Expedition 334, and include hemipelagic clay to silty clay material (Unit I) and pelagic silicic to calcareous ooze (Unit II). The frictional properties of the samples were tested at a normal stress of 5 MPa under water-saturated conditions and with slip velocities ranging from 0.0028 to 2.8 mm/s for up to 340 mm of displacement. The experimental results reveal that the steady-state friction coefficient values of clay to silty clay samples are as low as ~0.2, whereas those of silicic to calcareous ooze samples are as high as 0.6 to 0.8. The clay to silty clay samples show a positive dependence of friction on velocity for all tested slip velocities. In contrast, the silicic to calcareous ooze samples show a negative dependence of friction on velocity at velocities of 0.0028 to 0.28 mm/s and either neutral or positive dependence at velocities higher than 0.28 mm/s. Given the low frictional coefficient values observed for the clay to silty clay samples of Unit I, the décollement at the Costa Rica Seismogenesis Project transect offshore the Osa Peninsula likely initiates in Unit I and is initially very weak. In addition, the velocity-strengthening behavior of the clay to silty clay suggests that faults in the very shallow portion of the Costa Rica subduction zone are stable and thus behave as creeping segments. In contrast, the velocity-weakening behavior of the silicic to calcareous ooze favors unstable slip along faults. The shallow seismicity occurred at a depth as shallow as ~9 km along the Costa Rica margin offshore the Osa Peninsula ($M_w$ 6.4, June 2002), indicating that materials characterized by velocity-weakening behavior constitute the fault zone at the depth of the seismicity. Fault slip nucleating along a fault in Unit II would be a likely candidate for the source of the shallow earthquake event.

**Keywords:** Friction; Costa Rica; Earthquake; Subduction zone; $a - b$

## Findings

### Introduction

Subduction zone earthquakes exhibit spatial variability in seismic behavior along megathrusts, ranging from stable sliding or episodic slow slip events (SSEs) to large earthquakes (Ide et al. 2007). This variation likely reflects spatial variations in frictional properties along the seismogenic portion of plate-boundary megathrusts (e.g., Bilek and Lay 1998; Scholz 1998; Bilek 2007; Wang and He 2008; Rushing and Lay 2012).

An increasing number of experimental studies have found that the frictional properties of subduction-zone material vary depending on mineralogy, such as clay content, emphasizing the expected strong material control on frictional properties along seismogenic subduction zone thrusts (Vrolijk 1990; Brown et al. 2003; Kopf and Brown 2003; Ikari et al. 2009a; Ujiie and Tsutsumi 2010; Tsutsumi et al. 2011; Ikari et al. 2013; Saito et al. 2013; Takahashi et al. 2013; Ujiie et al. 2013). Given the diversity in subduction-

* Correspondence: tsutsumi@kueps.kyoto-u.ac.jp
[1]Department of Geology and Mineralogy, Division of Earth and Planetary Sciences, Graduate School of Science, Kyoto University, Kyoto 606-8502, Japan
Full list of author information is available at the end of the article

zone stratigraphy (Underwood 2007), it is essential to characterize the material inputs to subduction zones with respect to their intrinsic frictional properties if fault behavior within seismogenic subduction zones is to be better understood (Vrolijk 1990; Underwood 2007). However, available experimental data have thus far been limited mostly to clayey subduction-zone materials.

In this study, to explore variations in the intrinsic frictional properties of subduction zone sediment inputs that may be manifested in earthquake behavior along an erosional subduction zone interface, we examined the frictional properties of such sediments on the Cocos plate offshore the Osa Peninsula, Costa Rica. Our results reveal that variations in material inputs should produce variations in frictional properties along faults in the shallow Costa Rica subduction zone, providing an important constraint on faulting along the Costa Rica subduction zone interface.

## Geological setting

Along the Middle America Trench, offshore the western margin of Costa Rica, the oceanic Cocos plate is subducting beneath the Caribbean plate at a convergence rate of 70 to 90 mm/year, forming the southern end of the Middle America Trench (Protti et al. 1994; DeMets, 2001; Figure 1a). The Cocos plate subducting beneath Costa Rica was formed at two different spreading centers, the East Pacific Rise (EPR) and the Cocos-Nazca spreading center (CNS), and has been significantly influenced by Galapagos hotspot volcanism (von Huene et al. 2000; Barckhausen et al. 2001). The largest feature formed by the passage of the Cocos plate over the Galapagos hotspot is the 2.5-km-high Cocos Ridge (Figure 1).

The location of shallow earthquakes along the plate interface varies along strike: earthquakes occur shallower and closer to the trench in the CNS crust than in the EPR crust (Protti et al. 1994; Newman et al. 2002). In June 2002, a Mw 6.4 earthquake occurred at a depth as shallow as ~9 km along the Costa Rica margin offshore the Osa Peninsula (Arroyo et al. 2009). The subduction zone beneath the Caribbean plate is also characterized by strong variations in fault-slip behavior. Recently, the network of GPS stations around the Nicoya Peninsula has detected SSEs accompanied by seismic tremors in the Costa Rica subduction zone, not only at depths of 25 to 30 km near the down-dip limit of the seismogenic zone but also at depths of ~6 km near the up-dip limit (Outerbridge et al. 2010; Jiang et al. 2012). However, SSEs are not observed around the Osa Peninsula.

Integrated Ocean Drilling Program (IODP) Expedition 334, which also constituted a part of the Costa Rica Seismogenesis Project (CRISP), was established to understand the processes that control the nucleation and seismic rupture of large earthquakes along the Costa Rica erosive margin offshore the Osa Peninsula (Vannucchi et al. 2012). The primary objective of Expedition 334 was to both sample and quantify the sediment inputs to the seismogenic zone of an erosive subduction margin. In this expedition, Site U1381, which is located 50 km offshore the Osa Peninsula (Figure 1), is a key site for characterizing the material inputs to the subduction zone. The samples analyzed in the present study were recovered from this site.

## Experimental samples

All the samples tested in this study were collected from the sediments on the Cocos plate offshore the Osa Peninsula, at Site U1381, during IODP Expedition 334 (Figure 1a). The cores recovered from this site can be divided into three lithostratigraphic units (Figure 1b; Expedition 334 Scientists, 2012). The 95.57-m-thick cover sequence is divided into two units on the basis of lithology: Unit I is composed of clay to silty clay and Unit II is composed of silicic to calcareous ooze (Expedition 334 Scientists 2012). Underlying these sediments, Unit III consists mainly of pillow basalt (Expedition 334 Scientists 2012). A total of 29 tephra horizons are observed within the cover sediments (3 horizons in Unit I and 26 horizons in Unit II), with the tephra layers in Unit II being composed mostly of volcanic glass (Expedition 334 Scientists 2012). This study examined the frictional properties of four clay to silty clay samples (Unit I, Figure 2a), six silicic to calcareous ooze samples (Unit II, Figure 2c), and two tephra samples (tephras in Unit II, Figure 2b).

Biogenic components are observed in most of the samples. However, Unit II is distinguished from Unit I by its abundant biogenic components (Expedition 334 Scientists 2012). The clay to silty clay samples contain foraminifers, calcareous nannofossils, a few sponge spicules, and minor amounts of small silicic shells of organisms such as diatoms (Figure 2a). The silicic to calcareous ooze samples consist mainly of radiolarians, diatoms, silicoflagellates, sponge spicules, foraminifers, and calcareous nannofossils (Figure 2c). The tephra samples also include foraminifers and calcareous nannofossils.

Figure 2 shows X-ray diffraction (XRD) patterns obtained from the samples. The clay to silty clay samples consist of quartz, plagioclase, pyrite, phyllosilicate, and biogenic components. In contrast, the silicic to calcareous ooze samples of Unit II are almost free of clay minerals and are instead composed mainly of calcite and possibly amorphous silica. The existence of amorphous silica is indicated by a broad peak detected at $2\theta = 20°$ to 30°. The tephra samples also show similar broad peaks that indicate an abundance of glass.

## Experimental procedure

Friction experiments were conducted on the samples using a rotary-shear, intermediate- to high-velocity friction-testing machine. The collected samples were dried at 60°C

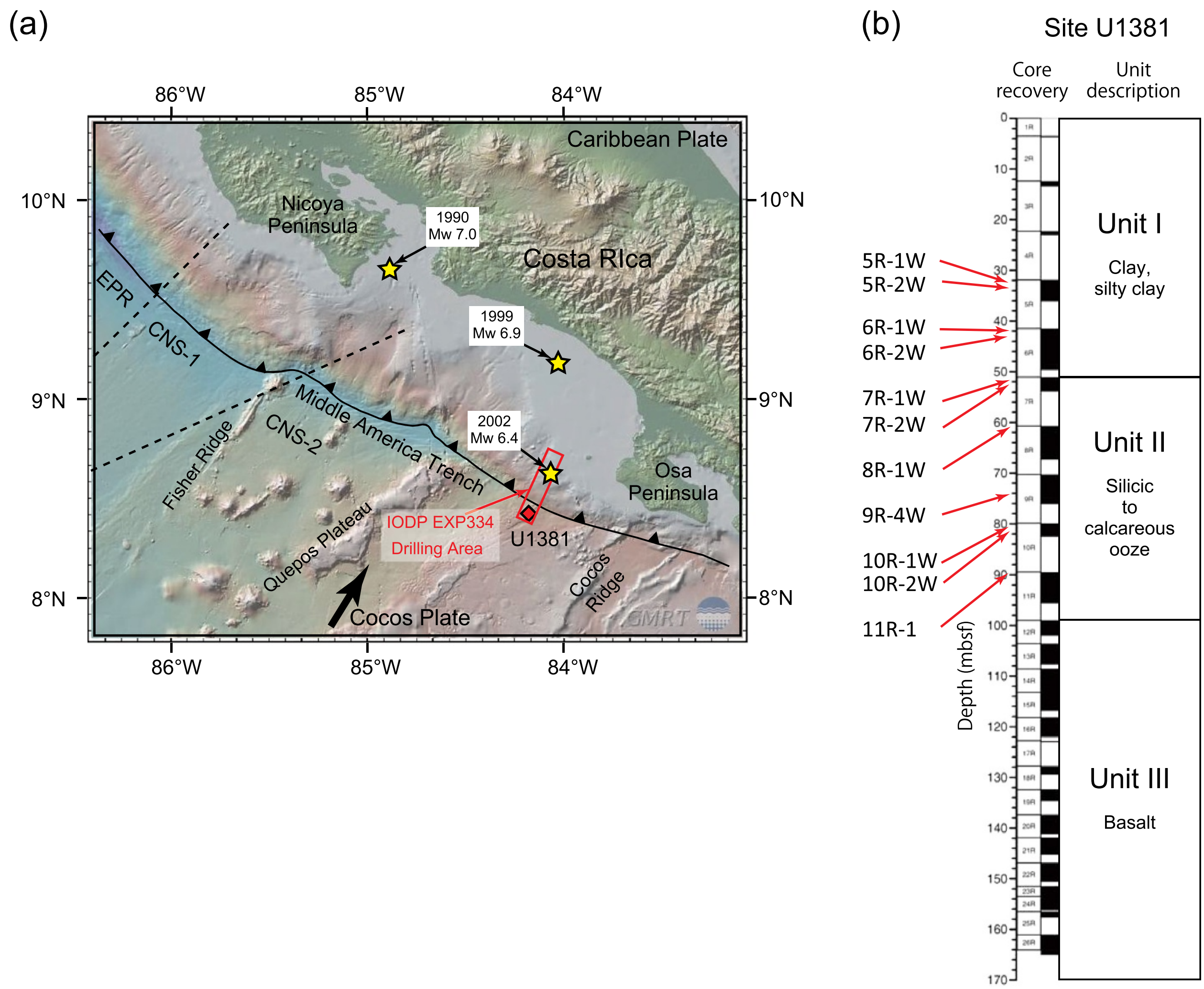


**Figure 1 Topographic and bathymetric map of the Costa Rica area and Hole U1381A summary. (a)** Topographic and bathymetric map of the Costa Rica area (Marine Geoscience Data System, MGDS; www.marine-geo.org; Ryan et al. 2009). The tectonic setting and major elements on the map are after Barckhausen et al. (2001). EPR, East Pacific Rise crust; CNS, Cocos-Nazca Spreading Center crust. Seismic event locations (stars) are from Arroyo et al. (2009). **(b)** Summary of the lithostratigraphy (after Expedition 334 Scientists 2012). Red arrows show the depth intervals of the core samples from which the experimental samples were taken. Sample 7R-2 W shows both white and black parts: the white part (7R-2 W white) can be classified in the silicic to calcareous ooze group, and the black part (7R-2 W black) in the tephra group.

for 24 h and disaggregated gently using a pestle. For each experiment, 0.5 g of the sample was placed between a pair of gabbro cylinders, each measuring 24.98 mm in diameter. Distilled water was added to the experimental gouge layer to saturate it. The experimental fault was surrounded by a Teflon® (DuPont, Wilmington, DE, USA) ring to avoid gouge expulsion during experiments. The gouge was axially pre-compacted under the test conditions (5 MPa) for 30 min.

In the friction experiments, all the pre-compacted samples were subjected to an initial slip velocity of 0.28 mm/s until ~170 mm of displacement (three rotations of the sample cylinder), during which time the friction value either increased or decreased to attain a roughly steady-state value. After this pre-sliding, a sequence of velocity stepping by a factor of 10 was imposed to examine the velocity dependence of friction for loading velocities of 0.0028 to 2.8 mm/s and displacements of >250 mm.

Velocity dependence was measured directly from plots of the data (e.g., Figure 3a,b,c,d) as the frictional constitutive parameter $(a - b) = (\Delta\mu_{ss}/\Delta \ln V)$ for a step change in sliding velocity using the first several hundred microns of displacement after the stepped velocity changes. As illustrated in Figure 3a,b,c,d, the response of friction to velocity steps is superimposed on longer-term gradual changes in friction, which occur over displacements of sometimes more than a few millimeters. These displacements are far

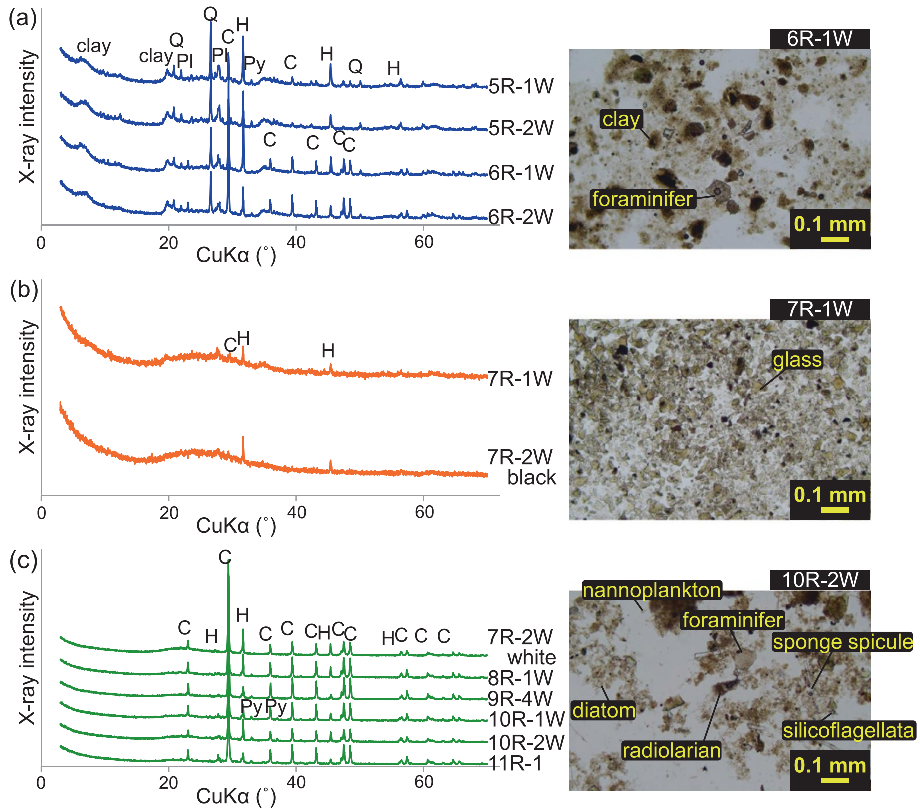


**Figure 2 XRD analysis and smear slide observation of the experimental samples.** XRD patterns of the tested samples and representative smear slide pictures of the samples. **(a)** Clay and silty clay. **(b)** Volcanic glass. **(c)** Silicic to calcareous ooze. Q, quartz; Pl, plagioclase; C, calcite; H, halite; Py, pyrite; clay, clay minerals.

larger than the typical critical weakening displacements reported for various gouge materials (e.g., Marone et al. 1990; Marone 1998). We interpret that such long-term behavior would likely be ascribed to the fluctuation in friction caused by the sample rotation, rather than to a transient frictional behavior modeled by the rate- and state-dependent friction laws (e.g., Dieterich 1979; Ruina 1983).

## Experimental results

The frictional behavior of the samples at a constant slip velocity $V$ of 0.28 mm/s differs between the samples of different lithostratigraphic units (Figure 4). For the clay to silty clay samples (Unit I), the friction coefficient $\mu$ is ~0.4 upon the onset of sliding, then gradually decreases over the initial 40 mm of sliding to attain a roughly constant value of ~0.15 (Figure 4b). In contrast, $\mu$ of the silicic to calcareous ooze samples is initially 0.4 to 0.6, then gradually increases to attain a roughly constant value of 0.6 to 0.8 (Figure 4c). The friction coefficient $\mu$ of the tephra samples is roughly constant within the range 0.6 to 0.8 over the entire displacement of the pre-sliding.

Figure 4a shows the initial peak and steady-state $\mu$ values measured for all the samples. The values of friction coefficient $\mu$ of the sediments at the onset of sliding at $V = 0.28$ mm/s, except for the tephra samples, are roughly in the same range of 0.4 to 0.6. In contrast, the steady-state $\mu$ values display clear differences between samples from different lithostratigraphic units. It is notable that the values of $\mu$ of the silicic to calcareous ooze samples decrease with greater sampling depth.

The samples tested in this study can be divided into two groups with regard to the velocity dependence of steady-state friction. Two representative results are shown in Figure 3a,c, in which $V$ was changed in a stepwise manner between 0.028 and 0.28 mm/s. Sample U1381A-6R-2 W (Figure 3a), representative of the clay to silty clay samples of Unit I, shows consistently positive velocity dependence at these velocities, whereas sample U1381A-8R-1 W (Figure 3c), representative of the silicic to calcareous ooze samples of Unit II, shows mostly negative velocity dependence. The critical slip distances $D_c$ at these velocities also differ between the two samples: the value of sample U1381A-6R-2 W is ~0.1 mm, whereas that of sample U1381A-8R-1 W is ~0.05 mm. At higher velocities of >0.28 mm/s, the velocity dependence of the clay to silty clay is still

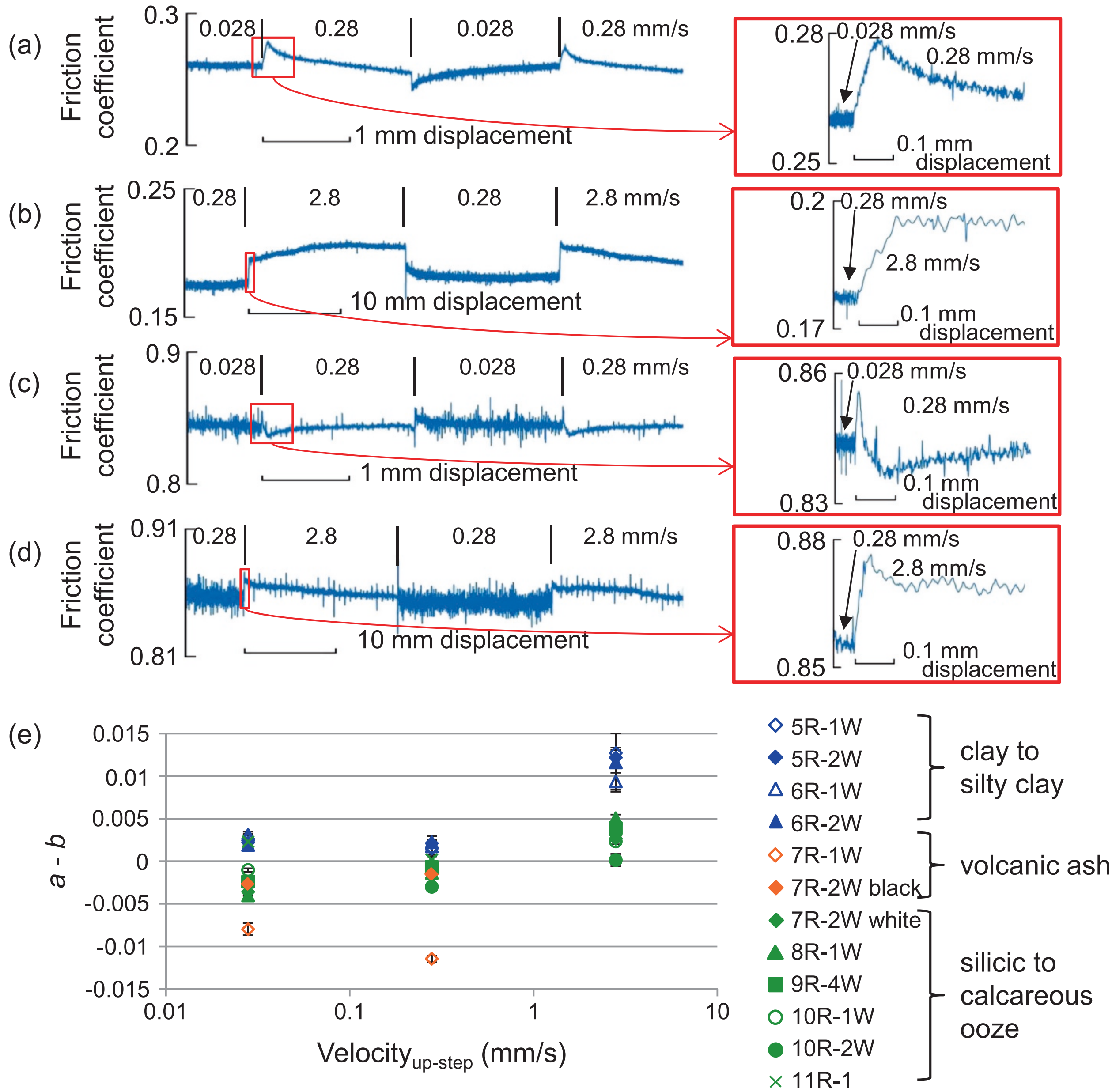


**Figure 3 Velocity dependence of friction measured by velocity-step tests.** Representative results of the velocity-step tests. **(a)**, **(b)** Sample U1381A-6R-2 W from Unit I (clay to silty clay) shows positive velocity dependence at $V = 0.028$ to 2.8 mm/s. **(c)**, **(d)** Sample U1381A-8R-1 W from Unit II (silicic to calcareous ooze) shows negative velocity dependence at $V = 0.028$ to 0.28 mm/s and positive velocity dependence at $V = 0.28$ to 2.8 mm/s. The inset figures show an enlarged plot for the duration of the velocity step. **(e)** Values of frictional velocity dependence of the tested samples for the range of sliding velocities $V = 0.0028$ to 2.8 mm/s.

positive (Figure 3b), whereas that of the silicic to calcareous ooze is either neutral or positive (Figure 3d).

Values of $(a - b)$ are plotted as a function of up-step velocities in Figure 3e. Values of $(a - b)$ of the clay to silty clay samples are low (<0.005) at lower velocities but increase to ~0.01 at the highest velocities. The absolute values of $(a - b)$ of the silicic to calcareous ooze samples are mostly low (<0.005) at the lowest velocities of 0.0028 to 0.028 mm/s. At intermediate velocities of 0.028 to 0.28 mm/s, absolute values of $(a - b)$ become smaller and approach zero, implying that the silicic to calcareous ooze samples exhibit an almost neutral velocity dependence of friction at these velocities (Figure 3e).

Similar contrasting frictional properties of subduction zone material have recently been reported by Ikari et al. (2013) from an experimental study of the sediments entering the Costa Rica subduction zone offshore the Nicoya Peninsula. In the Nicoya Peninsula region, calcareous

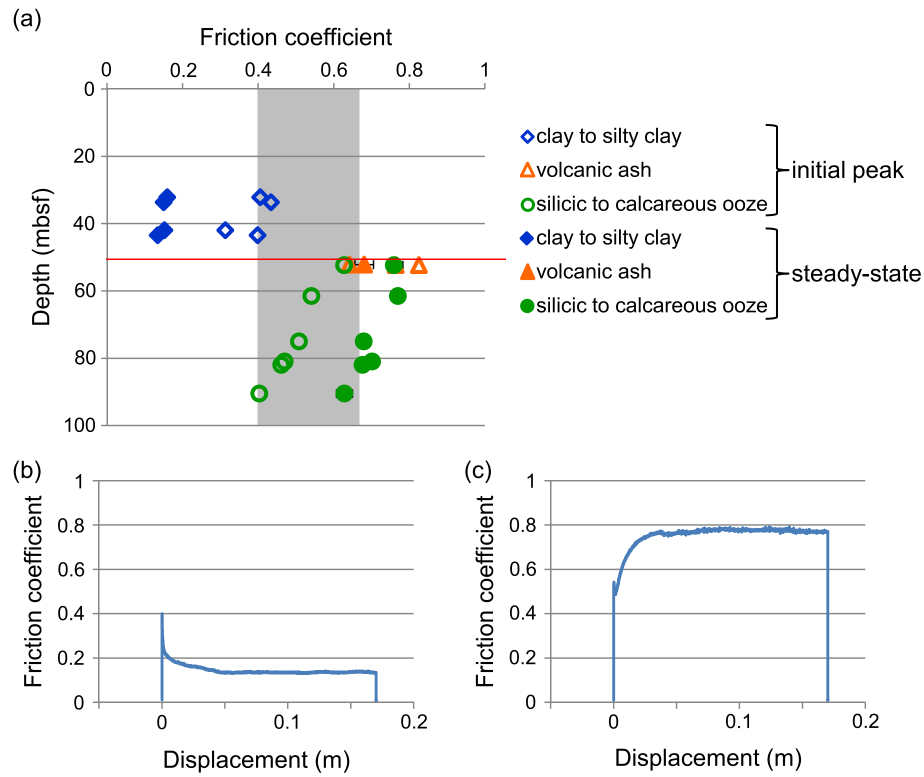


**Figure 4 Difference in shear strength between Unit I and Unit II sediments. (a)** Friction coefficient values (both initial peak and steady-state values) at constant velocity (0.28 mm/s) plotted against the depth intervals (mbsf) of the recovered core samples. **(b)**, **(c)** Evolution of the coefficient of friction with shear displacement for two representative samples: U1381A-6R-2 W (Unit I) and U1381A-8R-1 W (Unit II).

nannofossil chalk is frictionally strong ($\mu = 0.71$ to 0.88) and shows velocity-weakening behavior, whereas the hemipelagic clayey sediment is weak ($\mu = 0.22$ to 0.35) and exhibits mostly velocity-strengthening behavior.

## Discussion and conclusions

The observed weakness of the clay to silty clay sediments suggests that the frictional strength of faults is controlled mainly by the content of clay minerals, as has been demonstrated in many experimental studies (e.g., Summers and Byerlee 1977; Morrow et al. 1992, 2000; Brown et al. 2003; Kopf and Brown 2003; Moore and Lockner 2004; Ikari et al. 2009a,b; Tembe et al. 2010; Saito et al. 2013; Takahashi et al. 2013). In contrast, the steady-state $\mu$ values of the silicic to calcareous ooze sediments from Unit II are high, measuring ~0.8 and are comparable to the values reported for crustal rock samples (Byerlee 1978). The strength of the silicic to calcareous ooze samples probably arises because they are almost free of weak clay minerals.

The initial peak and steady-state $\mu$ values of the silicic to calcareous ooze samples decrease systematically with increasing depth (Figure 4a). No systematic change in physical properties (e.g., P-wave velocity, porosity, and shear strength) that would correlate to the variation in $\mu$ values has been reported for the Unit II cores (Expedition 334 Scientists 2012). However, it is interesting to note that some geochemical constituents of the pore fluid of the cores, such as the contents of Ca and $SO_4$, change monotonically with depth within Unit II (Expedition 334 Scientists 2012). This suggests the possible influence of fluid chemistry on the frictional properties of the fault material.

In the toe region of subduction zones, décollements are likely to initiate within, or shift their positions to, zones of weaker stratigraphic intervals (Underwood 2007). Given the low frictional coefficient values observed for the clay to silty clay samples of Unit I, the décollement at the CRISP transect offshore the Osa Peninsula likely initiated in Unit I and was initially very weak. It should be noted that our velocity-step tests reveal that clay to silty clay exhibits only positive frictional velocity dependence (Figure 3). The observed velocity-strengthening behavior and the very low steady-state $\mu$ values of the Unit I sediments suggest that the faults in the shallow portion of the Costa Rica subduction zone are stable and thus behave as creeping segments.

In contrast, the silicic to calcareous ooze samples from Unit II, which are characterized by higher $\mu$ values, exhibit mostly velocity-weakening behavior for slip velocities of

0.0028 to 0.28 mm/s (Figure 3e). Velocity-weakening behavior implies potentially unstable fault motion (Scholz 1998). In addition, the lower $D_c$ values of silicic to calcareous ooze samples may mean that faults that develop in Unit II are more unstable. The difference in $D_c$ values between Unit I and Unit II may be caused by different clay mineral contents. The June 2002 Mw 6.4 earthquake implies the existence of velocity-weakening material in this focal depth region. Fault slip that nucleated along a fault in Unit II would be a likely candidate for the source of the shallow earthquake event.

Variation in the distribution and type of earthquakes along the Costa Rica subduction zone, such as the shallow earthquake that occurred at Osa Peninsula (the 2002 $M_w$ 6.4 event, Figure 1a) and the SSEs at Nicoya Peninsula, is suggestive of variations in fault zone material along the plate interface. The simple stratification signature of the material inputs (Figure 1b) may help us to better understand the processes leading to a heterogeneous distribution of fault material along the subduction channel. For instance, the topography of the seafloor may contribute to generating a heterogeneous distribution of materials along the plate boundary (Ikari et al. 2013). Considering the possible association of seismicity with the dewatering reaction along the plate interface (e.g., Spinelli et al. 2006; Audet and Schwartz 2013), the stabilizing effect of pore fluid pressure in the vicinity of velocity-weakening faults must be taken into account. High pore fluid pressure may produce a conditionally stable region along a velocity-weakening fault with a small value of $(a - b)$ by reducing the effective normal stress (Scholz 1998). A velocity-weakening fault in Unit II would be stable under quasistatic loading but may become unstable under sufficiently strong dynamic loading. Velocity-strengthening behavior, as observed for the Unit II samples at higher velocities of 0.28 to 2.8 mm/s (Figure 3e), may also act to stabilize the propagation of earthquake ruptures, and may influence slip patterns along faults or the magnitudes of earthquakes. As suggested by Saito et al. (2013), such velocity-strengthening behavior, in addition to variation in pore fluid pressure, is important for understanding the behavior of faults in subduction zones.

#### Competing interests
The authors declare that they have no competing interests.

#### Authors' contributions
AT and KU obtained the samples and planned the experiments. YN and AT conducted the friction experiments. YN conducted the XRD analyses, and JK and YN analyzed the XRD data. YN and AT wrote the manuscript. All authors read and approved the final manuscript.

#### Acknowledgements
We thank two anonymous reviewers for their constructive comments and suggestions, which led to improvements in the manuscript. We used samples and data provided by the Integrated Ocean Drilling Program (IODP). We thank IODP Expedition 334 shipboard scientific personnel for the helpful discussions at various stages of this work. This research was supported by the IODP after-cruise research program, JAMSTEC, and MEXT grant 21107004. The study was also supported by MEXT Japan, under its Observation and Research Program for Prediction of Earthquakes and Volcanic Eruptions project. AT was supported partly by JSPS grant 24340104.

#### Author details
[1]Department of Geology and Mineralogy, Division of Earth and Planetary Sciences, Graduate School of Science, Kyoto University, Kyoto 606-8502, Japan. [2]Doctoral Program in Earth Evolution Sciences, Graduate School of Life and Environmental Sciences, University of Tsukuba, Tsukuba 305-0006, Japan. [3]Research and Development Center for Ocean Drilling Science, Japan Agency for Marine-Earth Science and Technology, Yokosuka 237-0061, Japan. [4]Department of Natural History Sciences, Faculty of Science, Hokkaido University, Sapporo 060-0810, Japan.

Received: 31 December 2013 Accepted: 4 July 2014
Published: 16 July 2014

#### References
Arroyo IG, Husen S, Flueh ER, Gossler J, Kissling E, Alvarado GE (2009) Three-dimensional P-wave velocity structure on the shallow part of the Central Costa Rican Pacific margin from local earthquake tomography using off- and onshore networks. Geophys J Int 179:827–849, doi:10.1111/j.1365-246X.2009.04342.x

Audet P, Schwartz SY (2013) Hydrologic control of forearc strength and seismicity in the Costa Rican subduction zone. Nat Geosci 6:852–855, doi:10.1038/ngeo1927

Barckhausen U, Ranero CR, von Huene R, Cande SC, Roeser HA (2001) Revised tectonic boundaries in the Cocos Plate off Costa Rica: Implications for the segmentation of the convergent margin and for plate tectonic models. J Geophys Res 106(B9):19207–19220, doi:10.1029/2001JB000238

Bilek SL (2007) Influence of subducting topography on earthquake rupture. In: Dixon TH, Moore JC (eds) The seismogenic zone of subduction thrusts. Columbia University Press, New York, pp 123–146

Bilek SL, Lay T (1998) Variation of interplate fault zone properties with depth in the Japan subduction zone. Science 281:1175, doi:10.1126/science.281.5380.1175

Brown KM, Kopf A, Underwood MB, Weinberger JL (2003) Compositional and fluid pressure controls on the state of stress on the Nankai subduction thrust: A weak plate boundary. Earth Planet Sci Lett 214:589–603, doi:10.1016/S0012-821X(03)00388-1

Byerlee J (1978) Friction of rocks. Pure Appl Geophys 116:615–626

DeMets C (2001) A new estimate for present-day Cocos-Caribbean plate motion: Implications for slip along the Central American Volcanic Arc. Geophys Res Lett 28(21):4043–4046, doi:10.1029/2001GL013518

Dieterich JH (1979) Modeling of rock friction 1. Experimental results and constitutive equations J Geophys Res 84:2161–2168, doi:10.1029/JB084iB05p02161

Expedition 334 Scientists (2012) Expedition 334 summary. In: Vannucchi P, Ujiie K, Stroncik N, Malinverno A (eds) Expedition 334 Scientists, Proc. IODP, 334. Integrated Ocean Drilling Program Management International, Inc, Tokyo, doi:10.2204/iodp.proc.334.101.2012

Ide S, Beroza GC, Shelly DR, Uchide T (2007) A scaling law for slow earthquakes. Nature 447(3):76–79, doi:10.1038/nature05780

Ikari MJ, Saffer DM, Marone C (2009a) Frictional and hydrologic properties of a major splay fault system, Nankai subduction zone. Geophys Res Lett 36, L20313, doi:10.1029/2009GL040009

Ikari MJ, Saffer DM, Marone C (2009b) Frictional and hydrologic properties of clay-rich fault gouge. J Geophys Res 114, B05409, doi:10.1029/2008JB006089

Ikari MJ, Niemeijer AR, Spiers CJ, Kopf AJ, Saffer DM (2013) Experimental evidence linking slip instability with seafloor lithology and topography at the Costa Rica convergent margin. Geology 41(8):891, doi:10.1130/G33956.1

Jiang Y, Wdowinski S, Dixon TH, Hackl M, Protti M, Gonzalez V (2012) Slow slip events in Costa Rica detected by continuous GPS observations, 2002–2011. Geochem Geophys Geosyst 13, Q04006, doi:10.1029/2012GC004058

Kopf A, Brown KM (2003) Friction experiments on saturated sediments and their implications for the stress state of the Nankai and Barbados subduction thrusts. Mar Geol 202:193–210, doi:10.1016/S0025-3227(03)00286-X

Marone C (1998) Laboratory-derived friction laws and their application to seismic faulting. Ann Rev Earth Planet Sci 26:643–696

Marone C, Raleigh CB, Scholz CH (1990) Frictional behavior and constitutive modeling of simulated fault gouge. J Geophys Res 95:7007–7025
Moore DE, Lockner DA (2004) Crystallographic controls on the frictional behavior of dry and water-saturated sheet structure minerals. J Geophys Res 109, B03401, doi:10.1029/2003JB002582
Morrow C, Radney B, Byerlee J (1992) Frictional strength and effective pressure law of montmorillonite and illite clays. In: Evans B, Wong TF (eds) Fault mechanics and transport properties of rocks. Academic, San Diego, California, pp 69–88, doi:10.1016/S0074-6142(08)62815-6
Morrow CA, Moore DE, Lockner DA (2000) The effect of mineral bond strength and adsorbed water on fault gouge frictional strength. Geophys Res Lett 27:815–818, doi:10.1029/1999GL008401
Newman AV, Schwartz SY, Gonzalez V, DeShon HR, Protti JM, Dorman LM (2002) Along-strike variability in the seismogenic zone below Nicoya Peninsula, Costa Rica. Geophys Res Lett 29(20):38-1–38-4, doi:10.1029/2002GL015409
Outerbridge KC, Dixon TH, Schwartz SY, Walter JI, Protti M, Gonzalez V, Biggs J, Thorwart M, Rabbel W (2010) A tremor and slip event on the Cocos-Caribbean subduction zone as measured by a global positioning system (GPS) and seismic network on the Nicoya Peninsula, Costa Rica. J Geophys Res 115, B10408, doi:10.1029/2009JB006845
Protti M, Güendel F, McNally K (1994) The geometry of the Wadati-Benioff zone under southern Central America and its tectonic significance: Results from a high-resolution local seismographic network. Phys Earth Planet Inter 84:271–287
Ruina A (1983) Slip instability and state variable friction law. J Geophys Res 88:10359–10370
Rushing TM, Lay T (2012) Analysis of seismic magnitude differentials ($m_b - M_w$) across megathrust faults in the vicinity of recent great earthquakes. Earth Planets Space 64:1199–1207, doi:10.5047/eps.2012.08.006
Ryan WBF, Carbotte SM, Coplan JO, O'Hara S, Melkonian A, Arko R, Weissel RA, Ferrini V, Goodwillie A, Nitsche F, Bonczkowski J, Zemsky R (2009) Global multi-resolution topography synthesis. Geochem Geophys Geosyst 10, Q03014, doi:10.1029/2008GC002332
Saito T, Ujiie K, Tsutsumi A, Kameda J, Shibazaki B (2013) Geological and frictional aspects of very-low-frequency earthquakes in an accretionary prism. Geophys Res Lett 40:703–708, doi:10.1002/grl.50175
Scholz CH (1998) Earthquakes and friction laws. Nature 391:37–42, doi:10.1038/34097
Spinelli GA, Saffer DM, Underwood MB (2006) Hydrogeologic responses to three-dimensional temperature variability, Costa Rica subduction margin. J Geophys Res 111, B04403, doi:10.1029/2004JB003436
Summers R, Byerlee J (1977) A note on the effect of fault gouge composition on the stability of frictional sliding. Int J Rock Mech Min Sci 14:155–160, doi:10.1016/0148-9062(77)90007-9
Takahashi M, Azuma S, Uehara S, Kanagawa K, Inoue A (2013) Contrasting hydrological and mechanical properties of clayey and silty muds cored from the shallow Nankai Trough accretionary prism. Tectonophysics 600:63–74, http://dx.doi.org/10.1016/j.tecto.2013.01.008
Tembe S, Lockner DA, Wong T-F (2010) Effect of clay content and mineralogy on frictional sliding behavior of simulated gouges: Binary and ternary mixtures of quartz, illite, and montmorillonite. J Geophys Res 115, B03416, doi:10.1029/2009JB006383
Tsutsumi A, Fabbri O, Karpoff AM, Ujiie K, Tsujimoto A (2011) Friction velocity dependence of clay-rich fault material along a megasplay fault in the Nankai subduction zone at intermediate to high velocities. Geophys Res Lett 38, L19301, doi:10.1029/2011GL049314
Ujiie K, Tsutsumi A (2010) High-velocity frictional properties of clay-rich fault gouge in a megasplay fault zone, Nankai subduction zone. Geophys Res Lett 37, L24310, doi:10.1029/2010GL046002
Ujiie K, Tanaka H, Saito T, Tsutsumi A, Mori JJ, Kameda J, Brodsky EE, Chester FM, Eguchi N, Toczko S, Expedition 343 and 343T Scientists (2013) Low coseismic shear stress on the Tohoku-Oki megathrust determined from laboratory experiments. Science 342:1211, doi:10.1126/science.1243485
Underwood MB (2007) Sediment inputs to subduction zones; why lithostratigraphy and clay mineralogy matter. In: Dixon TH, Moore JC (eds) The seismogenic zone of subduction thrusts. Columbia University Press, New York, pp 42–85
Vannucchi P, Ujiie K, Stroncik N, Malinverno A (2012) the Expedition 334 Scientists. In: Proc. IODP, 334. Integrated Ocean Drilling P Management International, Inc, Tokyo, doi:10.2204/iodp.proc.334.2012
von Huene R, Ranero CR, Weinrebe W (2000) Quaternary convergent margin tectonics of Costa Rica, segmentation of the Cocos Plate, and Central American volcanism. Tectonics 19(2):314–334
Vrolijk P (1990) On the mechanical role of smectite in subduction zones. Geology 18:703–707, doi:10.1130/0091-7613
Wang K, He J (2008) Effects of frictional behavior and geometry of subduction fault on coseismic seafloor deformation. Bull Seismol Soc Am 98(2):571–579, doi:10.1785/0120070097

doi:10.1186/1880-5981-66-72
**Cite this article as:** Namiki *et al.*: **Frictional properties of sediments entering the Costa Rica subduction zone offshore the Osa Peninsula: implications for fault slip in shallow subduction zones.** *Earth, Planets and Space* 2014 **66**:72.